A semi-empirical approach to link macroscopic parameters to microstructure of fibrous materials

P. Kerdudou, J.-B. Chéné, G. Jacqus, Camille Perrot, Sébastien Berger, P. Leroy

A semi-empirical approach to link macroscopic parameters to microstructure of fibrous materials

Pierre Kerdudou [a)]
Jean-Baptiste Chéné [b)]
Gary Jacqus [c)]
Laboratoire Européen d'Acoustique du Bâtiment, Centre Scientifique et Technique du Bâtiment, 84 avenue Jean Jaurès, Champs-sur-Marne, 77447 Marne-la-Vallée Cedex 2, France

Camille Perrot [d)]
Université Paris-Est, Laboratoire Modélisation et Simulation Multi Echelle, MSME UMR 8208 CNRS, 5 bd Descartes, 77454 Marne-la-Vallée, France

Sylvain Berger [e)]
Saint-Gobain Recherche, 39 Quai Lucien Lefranc, 93303 Aubervilliers, France

Pierre Leroy [f)]
Saint-Gobain Isover CRIR, BP 10019, 60291 Rantigny Cedex, France

At macro-scale, semi-phenomenological models are used to describe the acoustic behavior of porous materials. At micro-scale, manufacturers, familiar with a manufacturing process, have the ability to modify the microstructure of these materials. Establishing relationships between macroscopic model parameters and the characteristics of the microstructure is important, not only to improve our knowledge of the dissipation mechanisms, but also to optimize the materials through the manufacturing process. In this work, extensive measurements were performed on five glass wools for different manufacturing parameters. The macroscopic parameters were obtained by direct or indirect characterization methods and the microstructure described using SEM images. Measurement methods were then discussed and some of their limits identified for the specific case of fibrous materials. An abundant literature containing empirical or analytical relations exists to link microstructure and macroscopic parameters. Most of them were confronted with the measured data. Finally, analytical relations were selected to determine the porosity and the characteristics lengths from the density and the fiber diameters. Resistivity was provided with the same microstructure parameters according to an empirical relation. Regarding the tortuosity, tested formulas and measurements showed that this parameter was always close to unity for these materials and was therefore set to one.

[a)] email: pierre.kerdudou@cstb.fr
[b)] email: jean-baptiste.chene@cstb.fr
[c)] email: gary.jacqus@cstb.fr
[d)] email: camille.perrot@u-pem.fr
[e)] email: sylvain.berger@saint-gobain.fr
[f)] email: pierre.leroy@ saint-gobain.fr

1 INTRODUCTION

Fibrous materials are extensively used for their acoustic performance in building construction or transport industry. Physical properties of porous materials depend on micro-structure (constitutive materials and fibers arrangement). Manufacturers are familiar with a specific family of manufacturing processes, and have generally developed an experience which provides them an ability to modify the corresponding micro-structure. However, suitable models remain essential to understand and predict the effect of the associated microstructure modification on the acoustic behavior. Semi-phenomenological models provide a sufficiently detailed and robust description of the dissipation phenomena and can be confidently used for a wide range of porous materials. In this work, the classical Johnson-Champoux-Allard model[1-2] is therefore used as a basis at macro-scale with porosity, tortuosity, viscous and thermal characteristic lengths, and resistivity as input parameters. These measurable homogenized physicals quantities are connected to the material microstructure and used to express the equivalent dynamic density and the equivalent dynamic bulk modulus of porous materials. The aim of this paper is to link afore mentioned macroscopic parameters with the microstructure properties of fibrous material. Five different samples of glass wool are used to carry out this study. In the first part, their microstructure is described using measurements based on Scanning Electron Microscope (SEM) images; and some experimental estimates of the macroscopic parameters are obtained from direct and indirect measuring methods commonly used in the literature. We also briefly discuss some limits of these methods identified during the course of the characterization process when applied to highly porous fibrous samples. In the second part, macroscopic parameters are calculated from the microstructural data collected through SEM images when applying the relations extracted from a thorough review of the literature; and the corresponding results are compared with macro-scale measurements. A supplementary evaluation of the proposed semi-empirical approach is provided through a comparison of the sound absorption coefficient estimates obtained with the proposed semi-empirical model, direct measurements, and characterizations.

2 MATERIALS CHARACTERIZATION

2.1 Project overview

Five different glass wool samples, named 406, 407, 408, 409, and 410, and whose related manufacturing process characteristics were carefully selected throughout a pilot campaign, have been studied. These experimental products have the same thickness, the same constitutive material, and the same percentage of binder. Importantly, they are however differing throughout their process parameters: the mass density, the typical fiber length, and an index indirectly related to the class of fiber diameter. At micro scale, the glass fibers are assumed to me made from an isotropic solid material, with a mass density equal to the one of the glass. At macro scale, the glass wool samples can be considered as a transversely isotropic material from manufacturing process considerations. However, even at this later scale, the generally assumed homogeneity property might not always be verified. The uniform distribution of the fibers is an approximation, and local density differences are observed; Fig. 1 (b) and (c).

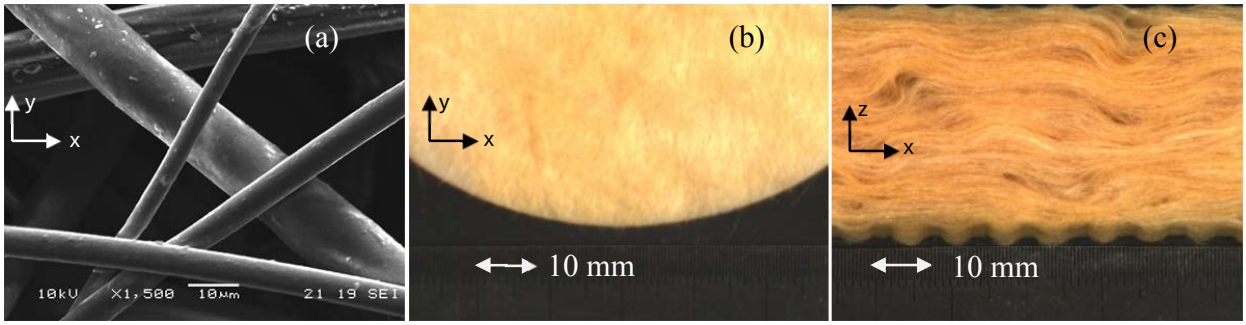

Fig. 1 – Multi-scale observation of a glass wool sample. (a) The micro-structure is revealed by employing scanning electro-micrographs. (b) Observation at macro-scale from the top of the sample seems compatible with a transversely isotropic assumption, at least at first approximation. (c) A transverse cross-section observation reveals that the so-called meso-structure is, however, not homogeneous, which induces local density differences.

2.2 Microstructure characterization

The micro-structure of the glass wool samples under study is analyzed from SEM images. Analyzed samples are coming from a 1200 mm × 600 mm glass wool panel. For each product, the number of image acquisitions is ranging between 700 and 1000. Results are presented in the form of log-normal distributions, together with the corresponding statistical parameters (arithmetic mean, median, log-normal mean).

Measurements are carried out by using ImageJ, a free image analysis software developed by the NIST. All pictures are taken from the top of the sample (xy plan); as in Fig 1(a)(b). This means that the micro-structure is essentially described through a two-dimensional (2D) analysis. Yet, this procedure does not allow a three-dimensional (3D) reconstruction of the material micro-geometry. To circumvent this difficulty, the glass wool samples are assumed to be made from successive layers of randomly distributed fibers. In other words, only two-directional random fiber structures having their axes on planes parallel to each other are considered in this investigation.

The magnification used for the acquisition of SEM images is ranging between 1000 and 1500 for measuring the fiber diameter d, whereas it is ranging between 100 and 500 to estimate the length L between two superposed fibers in the plane of observation; Fig. 2(left and right, respectively). In this work, the later estimate is only used to check if the validity of a dilute-like framework of fibers is verified in the 2D assumption. Note that the fibers are considered as straight cylinders having a circular cross-section shape.

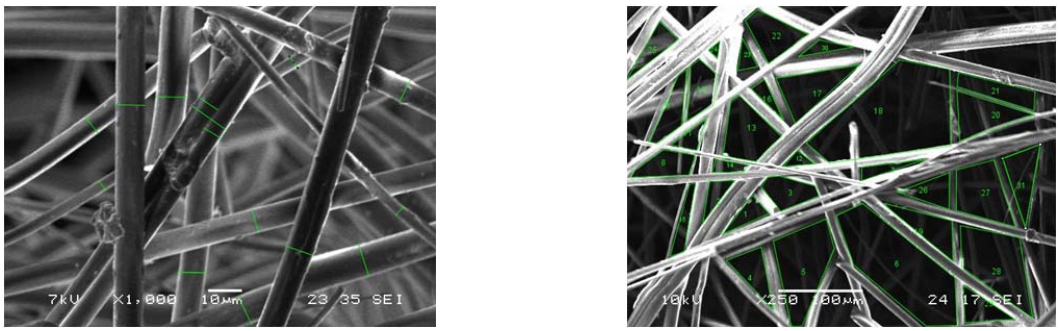

Fig. 2 – Fibers glass SEM images at different scales of observation. Superimposed straight lines are used to estimate the fiber diameters and the inter-connection lengths of the fibers network.

2.3 Macroscopic parameter measurement

Measurements of physical material properties were carried out at the acoustic laboratory of CSTB (LABE-European Laboratory of Building Acoustics). In this work, as previously mentioned in the introduction, the Johnson-Champoux-Allard model[1-2] is used, in which the material having a frame supposed to be rigid is replaced by an equivalent fluid. The equivalent dynamic mass density ρ_{eq} and the equivalent dynamic bulk modulus K_{eq} of the porous samples, two frequency-dependent and complex quantities, are derived in this model resistivity σ [Pa.s.m^{-2}], porosity Φ, tortuosity α_∞, viscous characteristic length Λ [m], and thermal characteristic length Λ'[m].

In the present study, the porosity is measured according the pressure-mass method proposed by Salissou and Panneton[3]. The resistivity is measured using a direct method according to the standard NF EN 29053. Characteristic lengths and tortuosity experimental estimates are provided using the indirect characterization method proposed by Panneton and Olny [4-5]. The equivalent dynamic density and the equivalent dynamic bulk modulus of the material are necessaries data to apply this method. They are measured using the three-microphone impedance tube method proposed by Utsuno *et al.*[6]. Inner diameter tube used is 42 mm and parameters are evaluated in the high frequency range (2000 – 4500 Hz) by averaging values in a specific frequency band where the parameters are relatively constants.

The sound absorption coefficient measurements are performed for a normal incidence, with an impedance tube, according to the standard NF EN ISO 10534-2.

3 REVIEW OF PREVIOUS WORKS REGARDING MICRO-MACRO LINKS

The porosity, defined as the ratio of the fluid volume V_f to the total volume V_t, is calculated[7] from the relative density ρ_r,

$$\rho_r = \frac{\rho_m}{\rho_s}, \tag{1}$$

where ρ_m is the equivalent density and ρ_s the density of skeleton .

A tortuosity estimate can be obtained by several empirical expressions developed for fibrous media. Some of them[8-9] need only the porosity as an input. Other authors used random-walk simulation results for the percolation threshold of randomly overlapping fiber structures[10-11] to derive the corresponding values of a generalization of Archie's law. Recently, an analytical relation was also developed[12] combining homogenization of periodic media and the self-consistent method for granular media consisting of a period array of spherical grains.

Many works were also developed to calculate the viscous permeability of fibrous media; the resistivity σ being related to the viscous permeability k_o and the viscosity of the fluid η by,

$$\sigma = \frac{\eta}{ko}. \tag{2}$$

Empirical models were mainly developed for synthetic fiber materials[13], or steel fibers stacking[14] from measurements and appropriate curve fittings, where the fiber diameter d is considered as a constant. *Ab-initio* simulations were also carried out from the lattice-Boltzmann method through large three-dimensional random fiber webs[15]. In this later work, each fiber was randomly oriented in the xy plane, and was then let to fall in the negative z direction until it made its first contact with the underlying structure. In these cases[13-14-15], the viscous permeability was obtained from porosity and fiber diameter. The thickness t of the sample is added in another work[16] to obtain more accurate results in the case of very thin synthetic fiber materials ($t < 3.5$ mm). According to these authors, the air resistivity experiments showed a significant effect of fiber web thickness on air permeability. We interpret these non-physical results as being due to a

significant relative compression of the samples under experimental conditions when having low fiberweb thicknesses. Indeed, the compression of the samples tends to orient the fibers in a direction perpendicular to the flow direction, which modifies the resistivity of the material and increases it artificially. In a remarkable paper, Tomadakis and Robertson[17] introduced the percolation threshold. Different fiber distribution orientations are studied and a method derived from electrical principles [1] is employed to predict the viscous permeability of the fibrous micro-structures. The percolation threshold value ε = 0.11 used in the present work corresponds to the two-directional randomly overlapping fiber structures case, similar to our microstructure characterization assumption when using SEM images. Bies and Hansen developed an empirical model for mineral wool samples[18] which provides directly the resistivity from the fibers diameter and the material density. Measurements were carried out on a large range of glass wool samples, and the typical fiber diameter is taken from an arithmetic mean of the collected data.

Allard and Champoux[19] proposed an analytical approach to obtain the viscous and thermal length for fibrous media from the calculation of the velocity field around a fiber with circular cross-section shape in the dilute limit (high porosity). Boutin and Geindreau[12-20] developed an analytical model to express characteristic lengths for granular media composed of spherical particles**.**

Formulas from all of these different works are summarized in Table 1.

Table 1 – Literature's formulas to link macroscopic parameters to microstructure

Macroscopic parameters	**Authors**	**Formula**	
Porosity	Gibson and Ashby, 1997 **[7]**	$\phi = \frac{V_f}{V_t} = 1 - \frac{\rho_m}{\rho_s} = 1 - \rho_r$	(3)
Tortuosity	Comiti and Renaud, 1989 **[8]**	$\alpha_\infty = 1 + 0.41 \ln\left(\frac{1}{\phi}\right)$	(4)
	Archie, 1942 **[9]**	$\alpha_\infty = \left(\frac{1}{\phi}\right)^{0.3}$	(5)
	Tomadakis and Sotischos, 1993 **[10]**	$\alpha_\infty = \left(\frac{1-\varepsilon}{\phi-\varepsilon}\right)^{0.785} \times \left(1 + \frac{0.785\phi}{\phi-\varepsilon}\right)^2$	(6)
	Koponen and al, 1998 **[11]**	$\alpha_\infty = 1 + 0.65 \times \frac{(1-\phi)}{(\phi-\varepsilon)^{0.19}}$	(7)
	Boutin and Geindreau, 2008 **[12]**	$\alpha_\infty = \frac{3-\phi}{2}$	(8)
Resistivity and viscous permeability	Davies, 1952 **[13]**	$k_0 = d^2\,[64 \times (1-\phi)^{\frac{3}{2}} \times (1 + 56 \times (1-\phi)^3)]^{-1}$	(9)
	Rahli and al,1995 **[14]**	$k_0 = \frac{62{,}5\,\phi^6 d^2}{(1-\phi)^2\ (3.6 + 56.4\,\phi)^2}$	(11)
	Koponen. and al, 1998 **[15]**	$k_0 = \frac{d^2}{4} 5{,}55[e^{10{,}1(1-\phi)} - 1]^{-1}$	(10)
	Vallabh and al, 2010 **[16]**	$k_0 = 6{,}82.10^{-6} \times d(1-\phi)^{-1} - 2{,}2.10^{-11} \times \ln(z) + 1{,}64.10^{-4} \times d(1-\phi)^{-2} - 1{,}71.10^{-9} * (1-\phi)6{,}66.10^{-10}$	(12)
	Tomadakis and Robertson, 2005 **[17]**	$k_0 = \frac{d^2\,\phi}{32 ln^2 \phi} \times \frac{(\phi-\varepsilon)^{0.785+2}}{(1-\varepsilon)^{0.785} \times [(0.785+1)\phi - \varepsilon]^2}$	(13)
	Bies and Hansen, 1980 **[18]**	$\sigma = \frac{3.18 \times 10^{-9}}{d^2 {\rho_m}^{-1.53}}$	(14)
Characteristics length	Allard and Champoux, 1992 **[19]**	$\Lambda' = \frac{\mathrm{d}}{2\rho r}$	(15)
		$\Lambda = \frac{\mathrm{d}}{4\rho r}$	(16)
	Boutin and Geindreau, 2010 **[20]**	$\Lambda' = \frac{2\phi \times (r(-\phi+1)^{\frac{1}{3}})}{3(1-\phi)}$	(17)
		$\Lambda = \frac{2\phi \times (3-\phi) \times (r(-\phi+1)^{\frac{1}{3}})}{9(1-\phi)}$	(18)

4 RESULTS AND VALIDATION

4.1 Microstructure data and macroscopic parameters measurements

Microstructure data can be presented as a log-normal distribution (defined by a mean and standard deviation of randomly values). In order to test micro-macro links, several statistical indicators were successively calculated: the arithmetic mean, the median, and the log-normal mean. An illustration of log-normal distribution for the fiber diameters (products 408) together with the studied statistical indicators is presented for each product in the Fig. 3.

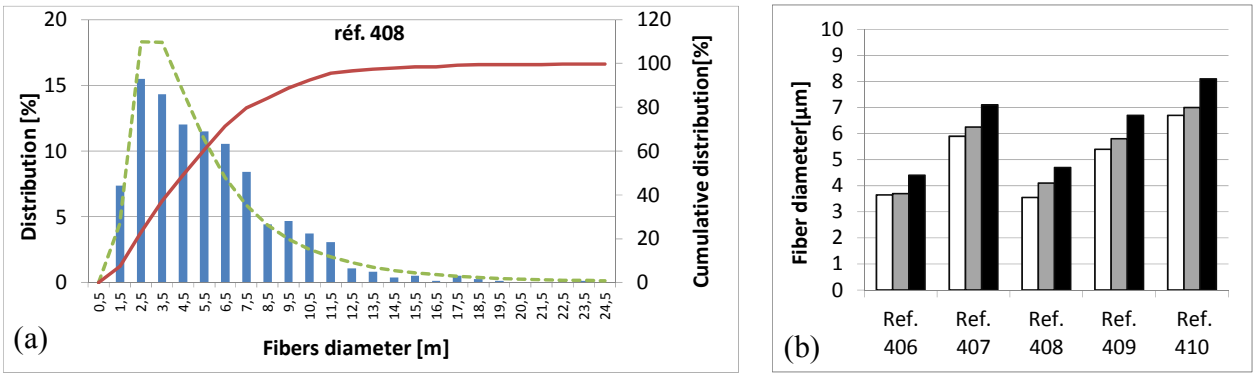

Fig. 3. Statistical representation of microstructural data. (a) Fiber diameters histogram (blue), associated cumulated distribution (red), and corresponding log-normal distribution (green). (b) Log normal mean (white), median (grey), arithmetic means (black) (b).

The statistical indicators illustrate the same trends whatever the products. It is shown that the arithmetic means of the fiber diameter always correspond to the highest values, whereas the data corresponding to the log-normal means are the lowest values. The lengths L between two superposed fibers in the plane of observation were measured for each product in order to check the model assumptions ($L >> d$). Measured results are presented in Table 2.

Table 2 – Microstructure data measurements

	Material density ρ_m **[kg/m^3]**	**Fiber diameter d [µm]**			**Length between fibers L [µm]**
		Log-normal mean	**Median**	**Arithmetic mean**	
406	20.07 ± 1.77	3.6 ± 0.5	3.7 ± 0.5	4.4 ± 0.5	51.7 ± 5
407	50.70 ± 0.98	5.9 ± 0.5	6.2 ± 0.5	7.10 ± 0.5	43 ± 5
408	49.7 ± 2.37	3.6 ± 0.5	4.1 ± 0.5	4.70 ± 0.5	27 ± 5
409	80.72 ± 2.57	5.4 ± 0.5	5.8 ± 0.5	6.70 ± 0.5	26 ± 5
410	51.60 ± 1.68	6.7 ± 0.5	7.0 ± 0.5	8.10 ± 0.5	36 ± 5

Table 3 – Macroscopic parameters measurements

	Material density ρ_m [kg/m^3]	**Porosity Φ [-]**	**Resistivity σ [Pa.s.m^{-2}]**	**Tortuosity α_∞ [-]**	**Viscous length Λ [μm]**	**Thermal length Λ' [μm]**
406	20.07 ± 1.77	0.987 ± 0.002	12500 ± 1300	1	75 ± 8	171 ± 44
407	50.70 ± 0.98	0.963 ± 0.004	32100 ± 1600	1	55 ± 3	84 ± 8
408	49.7 ± 2.37	0.967 ± 0.003	43100 ± 2400	1	46 ± 6	51 ± 7
409	80.72 ± 2.57	0.954 ± 0.002	90500 ± 5500	1	28 ± 2	70 ± 7
410	51.60 ± 1.68	0.962 ± 0.002	31300 ± 3500	1	53 ± 4	102 ± 12

Direct or indirect experimental methods introduced previously are used to characterize the macroscopic parameters of the wool sample under study. The tortuosity of all products is set to α_∞= 1, since the uncertainties of all the experimental results for this parameter is not enough accurate for the tested materials, and also because the simple value provide accurate enough predictions of the sound absorption coefficients for all the products. Table 3 presents the results of macroscopic parameters measurements. For all of these macroscopic parameters, a systematic comparison between the results obtained from model-dependent predictions and experimental data is presented and discussed.

4.3 Porosity

The method proposed by Salissou and Panneton[3] to measure the porosity of the glass wool samples is studied, but it should be mentioned that the corresponding results would lead to under-estimates. Indeed, simple calculations with typical operating conditions provide an upper limit of accessible porosity measurements (ϕ_{max}= 0.995). Moreover, it should be mentioned that at this degree of required accuracy, the experimental dimensions of the sample are not always easy to characterize. The geometry profile of the top and the bottom of the samples are not regular in shape.

The densities of the constitutive materials used to produce the glass wool samples under study are ρ_{glass} = 2540 kg/m^3 and ρ_{binder} = 1000 kg/m^3. The mass rates of the constituents are respectively equal to $Tx_{glass} = 95\%$ and $Tx_{binder} = 5\%$ for the glass and the binder according to the manufacturing process. Therefore, a more accurate porosity estimate of the glass wool sample is obtained from Eqn. (19),

$$\phi = 1 - \left(\frac{Tx_{glass}}{\rho_{glass}} + \frac{Tx_{binder}}{\rho_{binder}}\right) * \rho_m \,. \tag{19}$$

Then, the calculated porosity is compared to the measurements.

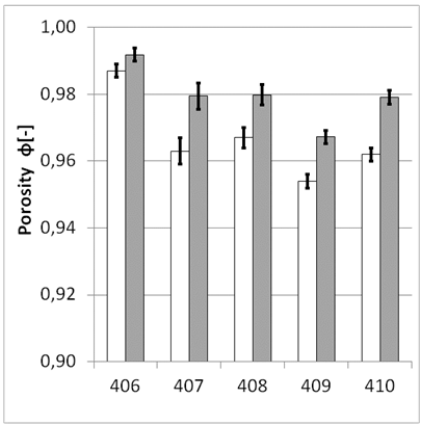

Fig. 3 –Measured (white) and calculated (grey) porosity

For all products, measured values of the porosity are always lower than the calculated ones (although differences are less than 2%).

4.4. Resistivity

Resistivity is calculated using Eqs. (2), (9), (10), (11), (12), (13), and (14) from experimental values of *d*, ρ_{glass}, and ρ_{binder}. Numerical applications of these relations show that the resistivity increases when the fiber diameter decreases.

Values of fiber diameter which provide the lowest differences when compared with measurement are selected for each model. The following figure shows the resistivity calculated error compared to the measurement for each model and the estimation of the resistivity for the most suitable models.

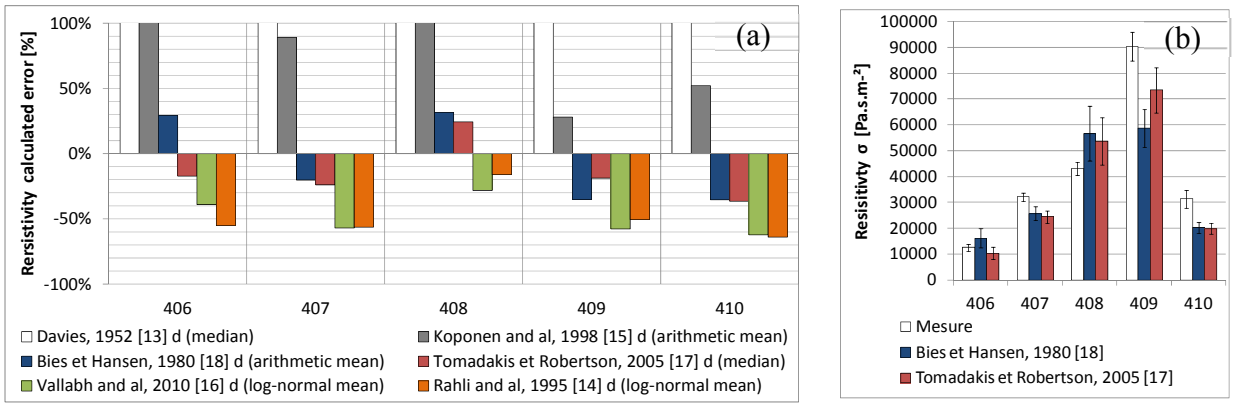

Fig. 4 –A comparison between calculated and measured resistivity for the studied empirical models (a), and a focus of the results obtained with Bies and Hansen and Tomadakis and Robertson models (b.)

Results from Fig. 4 shows that Davis[13] and Koponen *and al.*[15] models overestimate the prediction of the resistivity, whereas Vallabh *and al.*[16] and Rahly *and al.*[14] models underestimate the resistivity. Bies and Hansen[18] models using the value of the arithmetic mean fiber diameter provide a good estimate of this parameter, in agreement with authors' remarks. Also, the model proposed by Tomadakis and Robertson[17] using the median fiber diameter as an input data provides an excellent agreement with the measurements.

The static airflow resistivity is also determined using the extrapolation method in the low-frequency range on 42 mm diameter sample[4]. The results obtained according to this method are

comparable to the results provided by the direct method (NF EN 29053) using a 100 mm sample in diameter**.** In this work, indirect methods resistivity values were used to obtain an estimate of the tortuosity and the viscous characteristics lengths for each sample, because the glass wool inhomogeneity is better taken in account in this way and provide more accurate results.

4.5 Tortuosity

According authors remarks[4], an accurate tortuosity estimate is difficult when the resistivity of the porous medium is high. However, the tortuosity is always very close to unity.

The tortuosity is also calculated from the porosity using Eqs. (4), (5), (6), (7), (8) and provides results very close to one. All models show the same trends, tortuosity decreases for low porosity materials and all the values are ranging between 1 and 1.03. Comparisons between calculated and measured parameters are presented on the following figure.

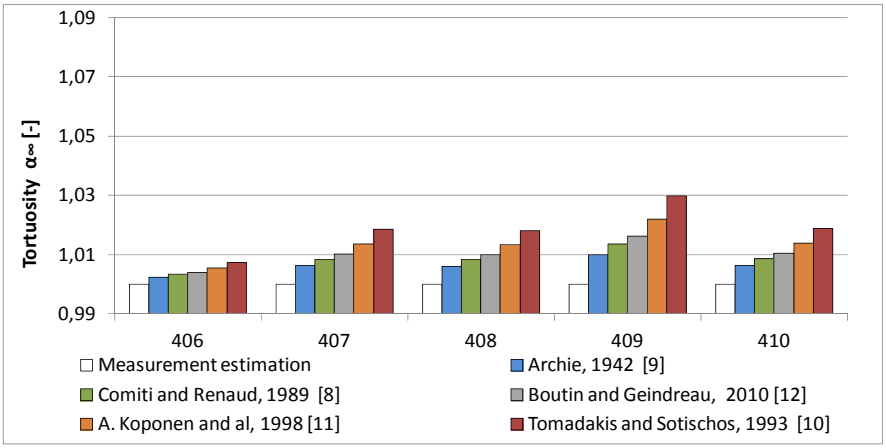

Fig. 3 –Tortuosity estimation from measures (white) and calculated tortuosity with different empirical models

The experimental estimation of the tortuosity is in excellent agreement with calculated values obtained using literature models, and showed that this parameter is always close to unity for the studied materials. Finally, tortuosity is set to one to estimate the viscous characteristic length in the next section of this paper.

4.6 Viscous and thermal characteristics lengths

The viscous length and thermal characteristic lengths were estimated in the following frequency ranges of interest: (2500 – 4500 Hz) and (3500 – 4500 Hz), respectively. The constancy of the determined parameters in a given frequency range assesses the validity of the equivalent fluid model used in this range. To avoid the influence of the frame vibration which generally occurs at medium frequencies, Iwase and al[21] proposed a method to minimize this phenomenon by inserting nails in the sample to be characterized. Olny and Panneton[5] have shown that the error caused by these additional nails is negligible, which allows a larger frequency band of interest in some cases.

Viscous and thermal lengths are calculated with Allard and Champoux[19] models using Eqs. (15) (16) and Boutin and Geindreau[12-20] models using Eqs. (17) (18). These analytical approaches show an increase in the values of the thermal and viscous lengths when the statistical indicator of fiber diameter increases. The log-normal mean fiber diameter value provides the better results. Boutin and Geindrau models overestimate thermal length and underestimate

viscous length for all tested materials. In agreement with the assumption of the models (i.e., fibrous media), the Allard and Champoux analytical model provides an excellent agreement with experimental results. This model requires that the distance between fiber interconnections is much large than the fiber diameter ($^{L}/_{d} > 10$). It should mentioned that measured microstructural data are as follows; $5 < {}^{L}/_{d} < 15$, which explains the differences observed in Fig. 5.

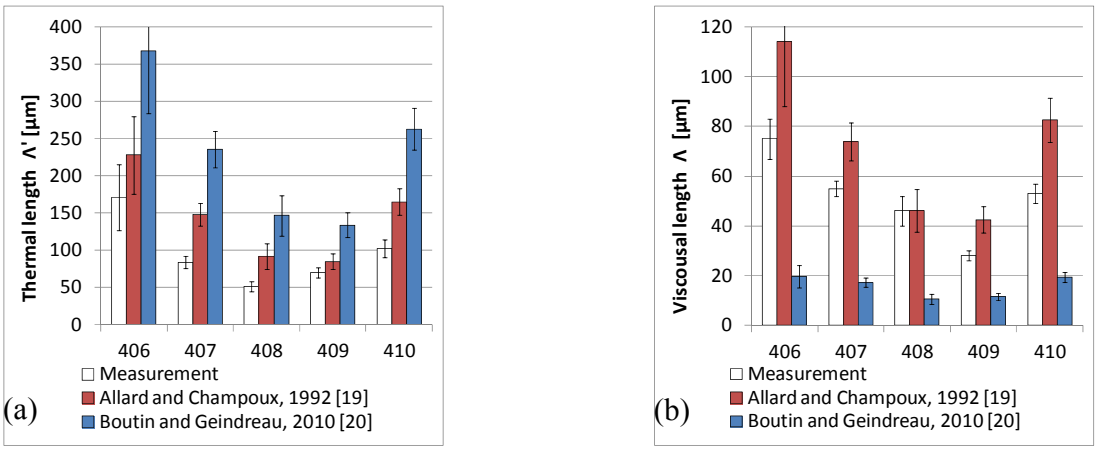

Fig. 5 –Measured (white) and calculated thermal lengths with Allard and Champoux model (red) and Boutin and Geindreau model (blue) (a). Measured (white) and calculated viscous lengths with Allard and Champoux model (red) and Boutin and Geindreau model (blue) (b).

4.7 Absorption coefficient

In order to validate the semi-empirical approach to link macroscopic parameters to microstructure of fibrous materials presented in this paper, absorption coefficient are estimated with measured and calculated macroscopic parameter. Porosity is calculated using. Eqn. (19), tortuosity is set to one, resistivity estimated using Eqn. (13), and characteristics lengths obtained using Eqs. (15) and (16). Calculations of the sound absorption coefficients at normal incidence of these glass wools follow from the classical Johnson-Champoux-Allard model.

A good prediction of the sound absorption spectrum is observed for all of these materials. We also note that when calculated macroscopic parameters are used, the main observed discrepancies related to the sound absorption coefficients are presumably due to the resistivity estimation errors related to the moderately high and high resistive materials (407, 408, 409 and 410 products). For the lowest resistive material (406), thermal characteristic length errors have also a significant impact on the predicted sound absorption coefficient.

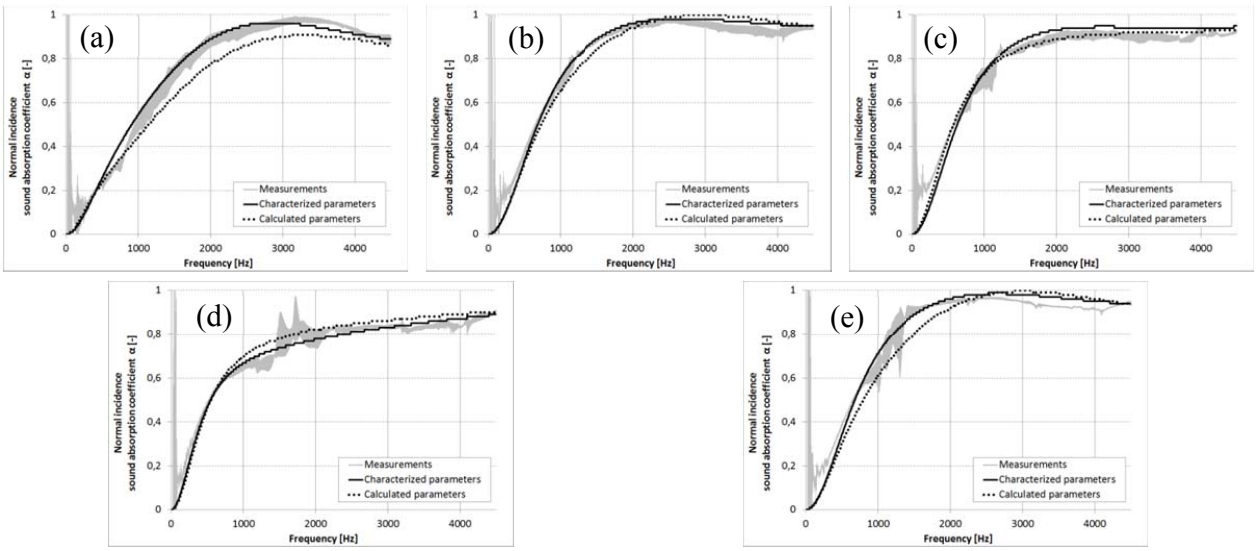

Fig. 6 –Measured (grey) and calculated absorption coefficient at normal incidence with measured macroscopic parameter (continuous line) and measured macroscopic parameter (dotted line) for material 406 (a), 407 (b), 408 (c) 409(d) and 410 (e)

4 CONCLUSIONS

In this experimental work, accurate predictions of the macroscopic parameters of real glass wool samples manufactured according to different local geometry parameters where given by properly selecting micro-macro relations from the literature, thereby linking the density of the fibrous materials and the fiber diameters to fundamental and physically measurable macroscopic parameters entering into the classical description of the sound absorbing behavior of acoustic materials. The main originality of this work is to provide an experimental characterization at both micro and macro scales of real fibrous microstructures used as soundproofing materials, and to show that simple relations of the literature can be used in order to describe the acoustical behavior of this class of porous media with an acceptable accuracy. Interestingly, experimental data collected throughout the course of this investigation might be used as a basis to test and evaluate further micro-macro relationships with a greater physical content without any adjustable constant. Future works should include a semi-automated acquisition of the fiber web microstructural features, and numerical homogenization calculations of all the macroscopic parameters entering into the sound absorption prediction of the three-dimensional arrangements of fibers corresponding to these real materials.

5 ACKNOWLEDGEMENTS

The authors gratefully acknowledge the CSTB Research and Development Department for financial support.

6 REFERENCES

1. D. L. Johnson, J. Koplik and R. Dashen, “Theory of dynamic permeability and tortuosity in fluid-saturated porous media”, J. Fluid Mech. 176, 379-402 (1987).
2. Y. Champoux and J. F. Allard, “Dynamic tortuosity and bulk modulus in air saturated porous media”, J. Appl. Phys. 70, 1975-1979 (1991).

3. Y. Salissou and R. Panneton, “Pressure/mass method to measure open porosity of porous solids”, J. Appl. Phys. 101, 124913 (2007).
4. R. Panneton and X. Olny, “Acoustical determination of the parameters governing viscous dissipation in porous media”, J. Acoust. Soc. Am. 119, 2027-2040 (2006).
5. X. Olny and R. Panneton, “Acoustical determination of the parameters governing thermal dissipation in porous media”, J Acoust. Soc. Am. 123, 814-824 (2008).
6. H. Utsuno, T. Tanaka, and T. Fujikawa, “Transfer function method for measuring characteristic impedance and propagations constants of porous meterials”. J Acoust. Soc. Am. 86, 637-643 (1989).
7. L.J. Gibson and M.F Ashby, “Cellular Solids-Structure and Properties”, 2nd ed. Cambridge University Press, Cambridge, 1997
8. J. Comiti and M. Renaud, “A New Model for Determining Mean Structure Parameters of Fixed Beds from Pressure Drop Measurements: Application to Bed Packed with Parallelepiped Particles”. Chem. Eng. Sci. 44, 1539-1545 (1989).
9. G. Archie, “The electrical resistivity log as an aid in determining some reservoir characteristics”, Transactions of AIME 146, 54-61 (1942).
10. M. M. Tomadakis and S. V. Sotischos, “Ordinary and transition regime diffusion in random fiber structure”, Am. Inst. Chem. Eng. J. 39, 397-412 (1993).
11. A. Koponen, M. Kataja, J. Timonen, D. Kandhai, “Simulations of single fluid flow in porous medium”, Int. J. Mod. Phys. C 09 , 1505-1521 (1998).
12. C. Boutin and C. Geindreau, “Estimates and bounds of dynamic permeability of granular media”, J. Acoust. Soc. Am. 124, 3576–3593 (2008).
13. D.N Davies, “The separation of airborne dust and particle”, Proc. Inst. Mech. Eng. 1, 185-194 (1952).
14. O. Rahli, L. Tardist, M. Miscevis, R. Santini, “Etude expérimentale des écoulements darcéens à travers un lit de fibres rigides empilées aléatoirement : influence de la porosité”, J. Phys. II France 5, 1739-1756 (1995).
15. A. Koponen, D. Kandhai, E. Hellén, M. Alava, A. Hoekstra, M. Kataja, K. Niskanen, P. Sloot, and J. Timonen “Permeability of three dimensional random fiber web”, Phys. Rev. Lett. 80, 716 – 719 (1998).
16. R. Vallabh and al, “New approach for determining tortuosity in fibrous porous media”, J. Eng. Fiber Fabr. 5, 7-15 (2010).
17. M.M Tomadakis and T.J Robertson, “Viscous permeability of random fiber Structures: comparison of electrical and diffusional with experimental and analytical results”, J. Comp. Mat. 39, 163-188 (2005).
18. D. A. Bies and C. H. Hansen, “Flow resistance information for acoustical design”, Appl. Acoust. 13, 357-391 (1980).
19. C. Boutin and C. Geindreau, “Periodic homogenization and consistent estimates of transport parameters through sphere and polyhedron packings in the whole porosity range”, Phys. Rev. E 82, 036313 (2010).
20. J.F Allard and Y. Champoux, “New empirical equations for sound propagation in rigid frame fibrous media”, J. Acoust. Soc. Am. 91, 3346-3353 (1992).
21. T. Iwase, Y. Izumi, and R. Kawabata, “A new measuring method for sound propagation constant by using sound tube without any air spaces back of a test material,” paper presented at Internoise 98, Christchurch, NewZealand, (1998).